Signal, Image and Video Processing (2021) 15:843–850
https://doi.org/10.1007/s11760-020-01805-1

ORIGINAL PAPER

SAR image despeckling method based on improved Frost filtering

Yang Pan[1] · Yinghui Meng[1] · Lei Zhu[1]

Received: 7 January 2020 / Revised: 13 September 2020 / Accepted: 14 October 2020 / Published online: 12 November 2020

Abstract
In this paper, a novel despeckling algorithm for synthetic aperture radar (SAR) images based on improved Frost filtering is proposed. A reconstructed decay factor which can better characterize the homogeneous and edge regions of SAR image is added into the Frost filter model by using the Lee filter coefficient to implement adaptively controlling the degree of filtering in different regions. The three-stage filtering strategy is performed for effective despeckling and edge preservation. The SAR image is pre-filtered by using the Frost filtering of the small window to obtain local statistics, and then the original SAR image is refine filtered twice utilizing these local statistical parameters. The two values are, respectively, biased toward smoothing and edge preservation by adjusting the variable constant and the window scales. Finally, the final filtering result is obtained by weighting the two filtering results with the reconstructed decay factor we proposed. The experiments demonstrate that compared with advanced approaches, the proposed method improves both despeckling and edge preservation ability.

Keywords Synthetic aperture radar · Image despeckling · Frost filtering · Three-stage filtering strategy · Reconstructed decay factor

1 Introduction

Synthetic Aperture Radar (SAR) has been extensively used in military and agricultural fields due to the advantages of high resolution, strong penetrability and all day all weather remote imaging. However, the SAR is a typical coherent imaging system [1] which coherently superimposes the echo signals of a large number of scattering points. Therefore, the random multiplicative speckle noise [2] is scattered on the obtained SAR image. The complexity and inhomogeneity of the speckle greatly affect the visibility, which increased in difficulty of the SAR image interpretation. Thus, the despeckling is a necessary preprocessing step in interpreting SAR data.

After decades of research and development, existing SAR image despeckling algorithms can be divided into three categories: spatial domain filtering, transform domain filtering, and partial differential diffusion filtering. Previous methods like Lee [3], Kuan [4] and the Frost [5] are the most representative spatial filtering methods. Such methods utilize the sliding window to estimate the local statistical features in the window, which can adaptively perform smoothing filtering and the calculation process is simple. However, it is greatly affected by the window scale and prone to noise residue or edge details blurred in the edge region. In 2005, Buades et al. proposed the famous non-local mean (NLM) filtering [6] for additive noise reducing. Then Dabov et al. proposed the BM3D [7] filtering algorithm which used the idea of non-local block matching. Afterward Sara and Chierchia, respectively, proposed SAR-BM3D [8] and MSAR-BM3D [9] algorithms based on BM3D for SAR image despeckling. Although this type of method has a significant improvement in speckle suppression performance, it is easy to generate pseudo-Gibbs stripes on the image. The application of non-local filtering in SAR images has proved its effectiveness, and the despeckling technique using non-local framework was soon proposed, including FANS [10], NL-CV [11] and NL-SAR [12].

The main idea of filtering methods based on the transform domain is to use its inherent properties to process the transform coefficients, so as to achieve the purpose of eliminating noise. Wavelet transform has the ability of multi-scale structure analysis and local time–frequency analysis, which is widely used in SAR image despeckling [13, 14]. In [15], curvelet is used to search for transform coefficients and this

✉ Yang Pan
panyang18203@126.com

Yinghui Meng
359961640@qq.com

[1] School of Electronic Information, Xi'an Polytechnic University, Xi'an 710048, China

modification in the transform domain improves the despeckling accuracy. The self-snake diffusion and sparse representation are combined in the contourlet domain [16], and finally the despeckled image is obtained by the inverse transformation. Tian proposed a despeckling method based on probabilistic generative model in nonsubsampled contourlet transform (NSCT) domain [17]. Although this transform domain-based despeckling technique works well on edge preservation, it requires a large amount of calculation and generates data redundancy.

Anisotropic diffusion filtering represented by classical SARD [18] algorithm and improved algorithm [19–21], which can control the direction and intensity of diffusion filtering to implement a good balance between the despeckling and the edge preservation. However, the algorithm is sensitive to the setting of the number of iterations and the time step, and it is easy to have the problem of image blur or incomplete despeckling of edge region during the iteration process.

In recent years, with the rapid development of deep learning technology and its extensive application in the field of image processing, SAR image despeckling algorithms based on deep learning [22, 23] have also emerged. Although this kind of methods can achieve satisfactory despeckling performance through the training process, it takes too long as a preprocessing step.

In this paper, according to the model of classic Frost and Lee filter model, we propose a reconstructed decay factor and apply it to the SAR image despeckling algorithm with a three-stage filtering strategy. Firstly, the SAR image is prefiltered by using the Frost filtering in a small window to obtain local statistical parameters, then the local statistical parameters are used to refine filter the original image twice in different kinds. By adjusting the variable constant coefficient and the window scales, two refined filtering results, respectively, giving priority to smooth and protecting edge details are obtained. Finally, the filtering result is obtained by weighting the two different refined filtering results using the reconstructed decay factor we proposed.

Following the Introduction, the rest of this paper is organized as follows. Section 2 analyzes the related work on conventional spatial despeckling. In Sect. 3, we describe the proposed algorithm with the reconstructed decay factor and three-stage filtering strategy. Section 4 illustrates the results of visual effect and parameter evaluation indexes in comparison with other despeckling algorithms. Finally, Sect. 5 draws conclusions.

2 Related work

Lee filtering is one of the typical methods for noise reducing using local statistical properties, which is based on the minimum mean square error (MMSE) estimation criterion. A window of a certain length is selected as the local area, and it is assumed that the a priori mean and variance can be obtained. Let the scene parameter s and the speckle noise n of the SAR image be independent of each other, and the observation value is f at the position $m = (x, y)$, the observation model of the SAR image is:

$$f(m) = s(m)n(m) \tag{1}$$

.

Then, the estimation model of the Lee filter is:

$$\hat{f}(m) = [1 - \lambda(m)]\overline{f}(m) + \lambda(m)f(m) \tag{2}$$

where $\hat{f}$ is the estimated value of weighted filtering, and the λ is the filter coefficient:

$$\begin{aligned}\lambda_{Lee} &= \arg\min E\left\{\left(\bar{s}(m) - s(m)\right)^2\right\} \\ &= \frac{\mathrm{var}\{s(m)\}}{\mathrm{var}\left\{s(m) + \bar{s}(m)\right\}\sigma_n^2}\end{aligned} \tag{3}$$

$\overline{s}$ is mean of the scene parameter s, σ_n^2 is the variance of the speckle; var{} represents the calculation of the variance. A variant form of Lee filter coefficient is obtained by deriving the deformation of formula (3), as shown in formula (4):

$$\lambda_{Lee} = \left[C_n^4(m) + C_n^2(m)\right] \Big/ \left[C_n^4(m) + C_f^2(m)\right] \tag{4}$$

where the $C_n(m)$ and $C_f(m)$ are, respectively, the coefficient of variation of the speckle noise $n(m)$ and the observation value $f(m)$ at the position m.

By analyzing Eqs. (2) and (3), the main idea of Lee filter to implement despeckling is based on local mean and variance of the image. If the pixel f of image is located in the homogeneous region, the local variance of the scene parameter s is small, then λ_{Lee} approaches 0, and the estimated value of the scene parameter is mainly determined by the local mean within the window, so the Lee filtering will maximize the smooth filtering of the homogeneous region of the image. Conversely, if the pixel of image f is located in a heterogeneous region, the local variance of the scene parameter s is large, and the filter coefficient λ_{Lee} is close to 1, then the estimated value is determined by the observation value f. Therefore, the degree of smoothing filtering is small and the noise residual is serious in the edge and strong texture region.

According to the local statistics in a sliding window, the Frost filter works on preserving the edges while reducing the speckle. Unlike the Lee filtering algorithm, Frost filtering adds a priori information of the scene parameters and is a

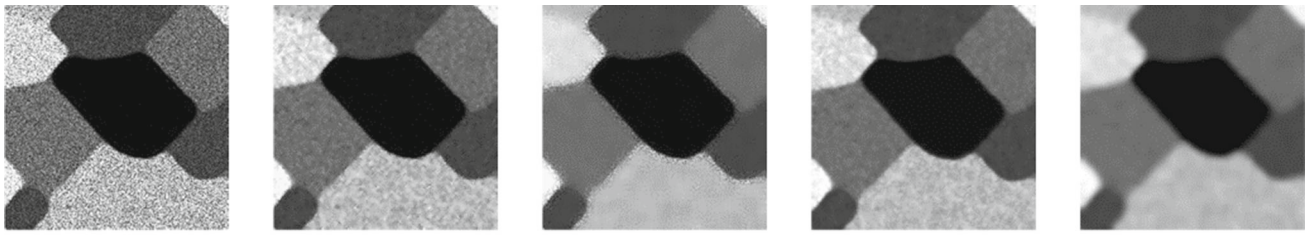

(a) (b) (c) (d) (e)

Fig. 1 Comparison of despeckled images by Lee filtering and Frost filtering under different parameters. **a** Synthetic SAR image. **b** Lee filtering in small window. **c** Lee filtering in large window. **d** Frost filtering with large α. **e** Frost filtering with small α

negative exponential weighting filter. The model can be given as:

$$\hat{f}(m) = \frac{1}{D}\sum_{r\in H} f(m+r)\exp(-\varphi(m+r)|r|) = \frac{1}{D}\sum_{r\in H} f(k)\exp(-\varphi(k)|r|) \quad (5)$$

In order to express the formula conveniently, set $k = m+r$ which represents the absolute position of other pixels, and the normalized factor D can be given as:

$$D = \sum_{r\in H}\exp(-\varphi(k)|r|) \quad (6)$$

and $|r|$ is the distance from the other pixels in the local window to the central pixel m.

The Decay factor $\varphi(k)$ is the crucial part in controlling the smoothness of the filter and defined as:

$$\varphi(k) = \alpha\sigma_f(k)\Big/\overline{f(k)} = \alpha C_f(k) \quad (7)$$

$\overline{f(k)}$ and $\sigma_f(k)$, respectively, represent the local mean and standard deviation of the pixel observation f at the position m in the window. The α is the variable constant, and $C_f(k)$ is the coefficient of variation which is a fixed parameter of the image and is only relevant to the image itself. If the value of α is large, the decay factor is large and the degree of speckle suppression is low, resulting in that the edge information remains intact but much noise residues. On the contrary, if the value of α is small, the result is reversed. The contrast between the two types of filtering under different parameters is illustrated in Fig. 1.

3 Proposed method

The original Frost filtering adopts a negative exponential weighting form, and its weight is determined by the coefficient of variation of the observation value and the distance from other pixels in the window to the central pixel. Through the filtering process, the degree of despeckling is not considered from the statistical characteristics of the speckle distribution, so the excess-filtering or deficient-filtering is easy to occur. By analyzing the estimation model of Lee filter, which has the characteristic of selective despeckling. According to the statistical characteristics of speckle in the local window, the homogeneous and heterogeneous regions are divided, thus enhance smoothness in homogeneous regions simultaneously reduce the degree of filtering through heterogeneous regions to retain edges.

Aiming at the problem that conventional Frost filtering cannot adaptively control the filtering degree, an improved method using the reconstructed decay factor with a three-stage filtering strategy is proposed.

3.1 Reconstructed decay factor

From the formula (7) of Sect. 2, the value of decay factor $\varphi(k)$ of Frost filter can be determined by the decay constant α, which demonstrate the original decay factor cannot adaptively change with image region. Through analyzing the formula (4), the weighting coefficient of Lee filter gives consideration to both observed value and speckle, which has the characteristic of selective filtering. Therefore, the reciprocal of Lee filter coefficient is added into the decay factor of Frost filter to effectively prevent the edge details from being excessively smoothed. According to the formula (4), the adaptive decay coefficient is formed as follows:

$$\mu(k) = 1\Big/\lambda(k) = \left[C_n^4(k) + C_f^2(k)\right]\Big/\left[C_n^4(k) + C_n^2(k)\right] \quad (8)$$

Due to the values of $C_f(k)$ and $C_n(k)$ are close in homogeneous area, then the $\mu(k)$ is close to 1. In the edge region, the value of $C_n(k)$ is much smaller than the $C_f(k)$, then the $\mu(k)$ is obviously larger than 1. Thus, $\mu(k)$ can adaptively change with the image region to take into account both despeckling and edge-preserving. The reconstructed decay factor is given as:

$$\psi(k) = \alpha\mu(k)C_f(k) \quad (9)$$

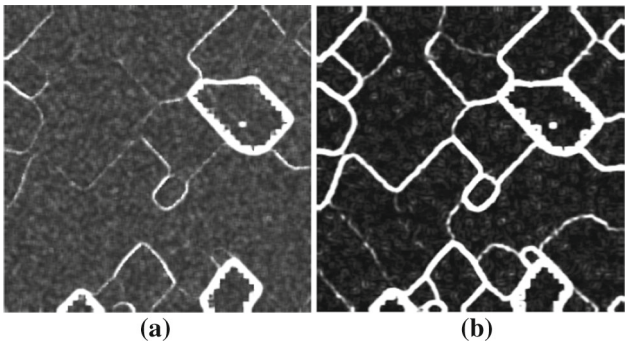

Fig. 2 **a** Decay factor of original Frost filtering. **b** Reconstructed decay factor

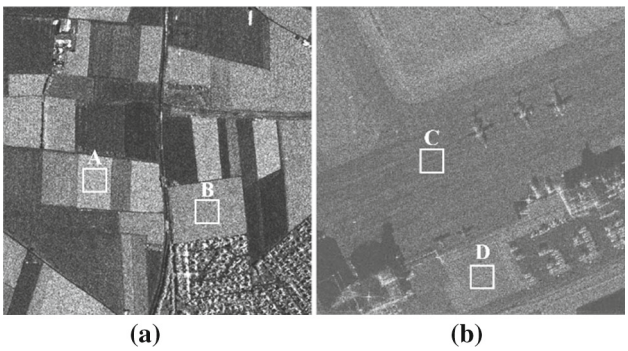

Fig. 3 Real SAR images. **a** Farmland. **b** Airport

The final negative exponential weighting coefficient of Frost filter as:

$$e^{-\psi(k)\,|r|} = e^{-\alpha\mu\,(k)\,C_f(k)\,|r|} = e^{-\alpha\,\frac{C_f(k)}{\lambda(k)}\,|r|} \tag{10}$$

Consequently, the improved Frost filter with reconstructed decay factor can adaptively control the degree of filtering in different regions. The difference between the original Frost filter decay factor and the reconstructed decay factor is given as Fig. 2.

3.2 Three-stage filtering strategy

The despeckling algorithm in this paper adopts a three-stage filtering strategy. First, the original image is pre-filtered once, then it is fine-filtered twice using different parameters. Finally, the final filtering result is obtained by weighting the two fine-filtered results using reconstructed decay factor.

Although the pre-filtering and the fine filtering have the same calculation process, the scales of weighted filtering window and the estimation objects of the local statistical parameters are different. The pre-filtering estimates the local statistical parameters of the original SAR image f, and the fine filtering implements the local statistical parameter estimation on the pre-filtered SAR image f_{pre}. Figure 4 illustrates the algorithm flow description, and the calculation process in detail is given as follows:

1. Several local statistics of original SAR image f are estimated by using small-scale window, as coefficient of variation of observed value C_f and distance parameter $|r|$. SAR image is filtered by original negative exponential weighting coefficient of Frost filter to weaken the speckles and get more accurate parameters. Then, the pre-filtered image f_{pre} is obtained.
2. Estimate multiple local statistics of the pre-filtered image f_{pre} using a large scale window, as Lee filter coefficient λ, coefficient of variation of observed value C_f

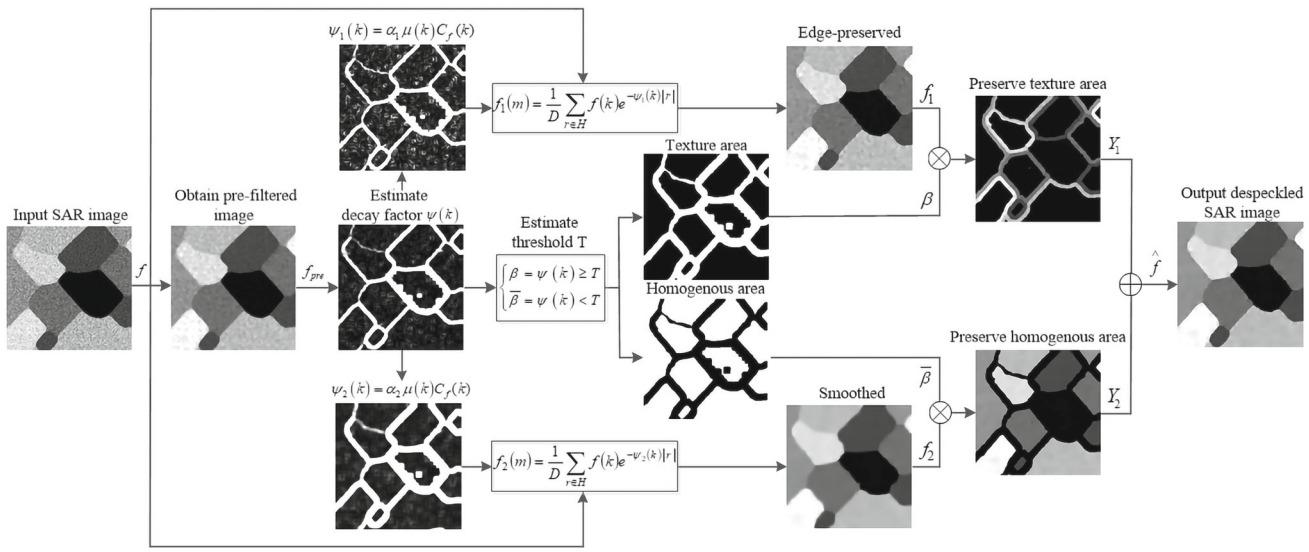

Fig. 4 Flowchart of proposed method

and distance parameter $|r|$.The original SAR image is filtered by a negative exponential weighting coefficient containing the reconstructed decay factor estimated of the pre-filtered image f_{pre}. According to Sect. 2 and Fig. 1, it can be seen that if α is smaller and the window scale is larger, the smoothing effect is more obvious; on the contrary, the edge preservation effect is better. Therefore, the two fine-filtered images f_1 and f_2 is obtained by adopting the appropriate window scales and variable constant α.

3. Finally, the final despeckled image $\hat{f}$ is obtained through performing the weighted sum of two different fine-filtered results f_1 and f_2 using the threshold T of $\psi(k)$. The reconstructed decay factor is divided into two values β and $\bar{\beta}$ by greater than and less than the threshold T. The threshold here is an empirical value obtained by evaluating the magnitude of the edge value of $\psi(k)$. Combining with the flowchart, the final filtered result can be expressed by the following formula.

$$\hat{f} = Y_1 + Y_2 = f_1\beta + f_2\overline{\beta} \tag{11}$$

4 Experimental results

In order to evaluate the speckle suppression and edge preservation performance of the proposed method, it is compared with SAR-BM3D [8], MSAR-BM3D [9], NL-CV [11] and IDPAD [20], which includes visual effects, parameter indexes and calculation analysis.

4.1 Visual effect evaluation

In this section, two real SAR images are used which are farmland and airport as shown in Fig. 3. The visual effects and edge detection graphs of the despeckling images of each algorithm are shown in Figs. 5, 6.

Aiming at objectively reflecting the best performance of despeckling and edge preservation of each algorithm, the optimal parameters are set based on the references of these comparison algorithms for two real SAR images. As for the algorithm in this paper, the parameters are set as follows,

1. For Fig. 3a, the local window and search window of pre-filtering are 3×3. The size of local window used to estimate Lee filtering coefficient is 9×9. The search window, local window, and decay constant of fine- filtering for smoothing and edge-preserving are, respectively, 9×9, 7×7, 1.5 and 5×5, 5×5, 3.6. The edge detection images are obtained by using Canny operator, and its threshold is 0.08.

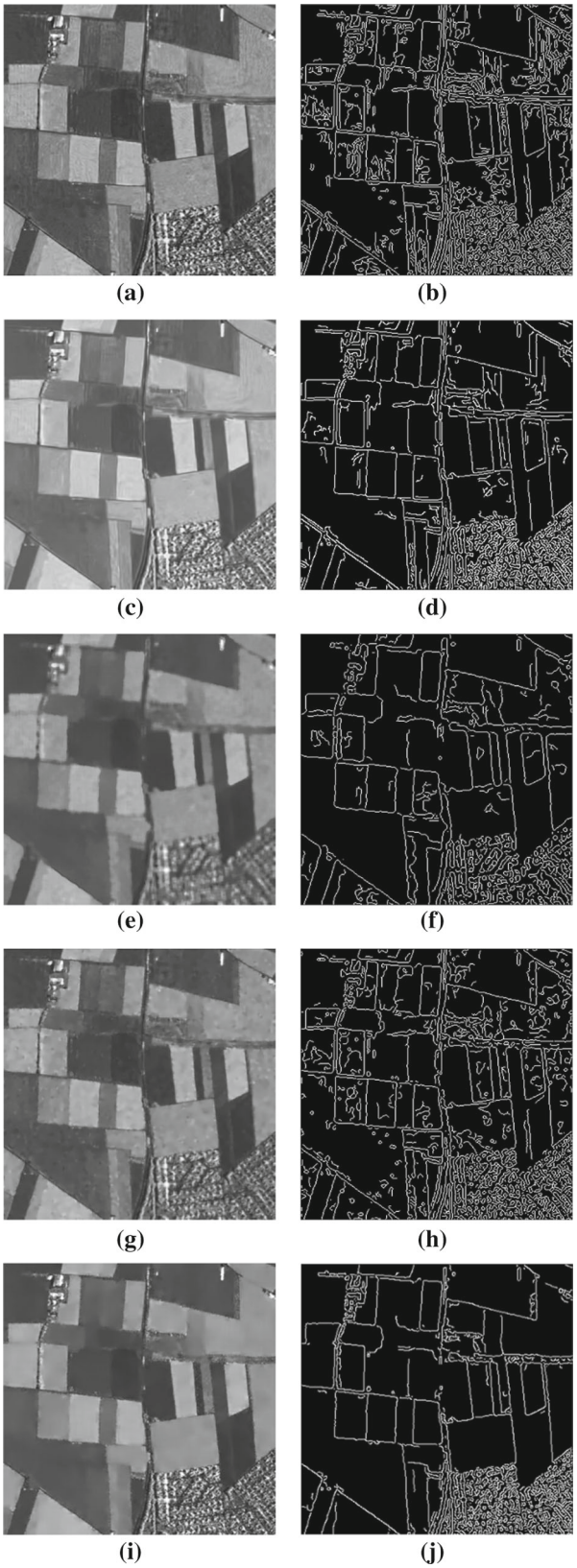

Fig. 5 Farmland SAR image despeckling and edge detection results for **a**, **b** SAR-BM3D. **c**, **d** MSAR_BM3D. **e**, **f** NL-CV. **g**, **h** IDPAD. **i**, **j** Proposed method

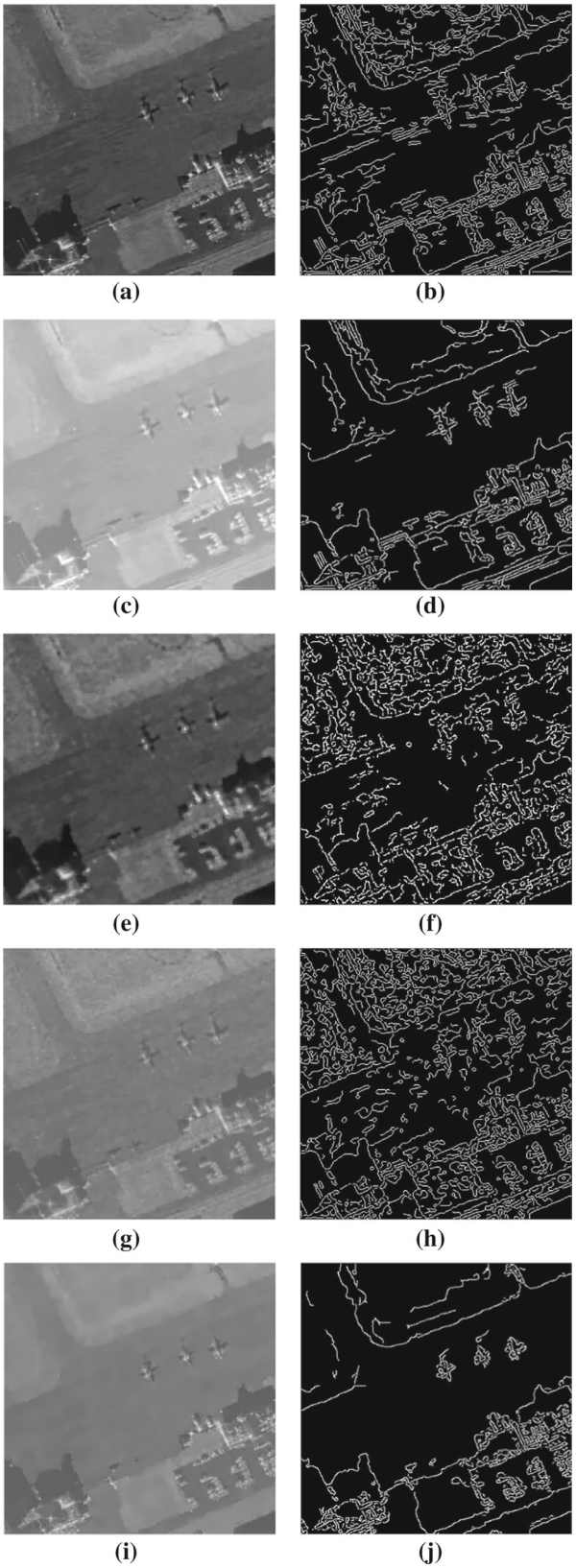

Fig. 6 Airport SAR image despeckling and edge detection results for **a**, **b** SAR-BM3D. **c**, **d** MSAR_BM3D. **e**, **f** NL-CV. **g**, **h** IDPAD. **i**, **j** Proposed method

2. For Fig. 3b, the local window and search window of pre-filtering are 3×3. The size of local window used to estimate Lee filtering coefficient is 7×7. The search window, local window, and decay constant of fine filtering for smoothing and edge-preserving are, respectively, 9×9, 7×7, 2.5 and 5×5, 5×5, 11. The edge detection images are obtained by using Canny operator, and its threshold is 0.08.

According to Figs. 5 and 6, it can be observed that the homogeneous region of proposed algorithm is smoother than other algorithm, further there is no pseudo-Gibbs fringe in SAR-BM3D and MSAR-BM3D algorithms. Comparing with the experimental results of IDPAD and NL-CV, the despeckling effect of proposed algorithm is more sufficient. Through the edge detection map of the despeckled images that the boundary of the proposed algorithm is clearer, and it is less likely that the noise is misinterpreted as a false edge.

4.2 Parameters evaluated indexes

The evaluation indexes used in this paper adopt Equivalent Number of Looks (V_{ENL}) and Edge Perseveration Index (V_{EPI}). These metrics are defined as:

$$V_{ENL} = \alpha \frac{\mu_A^2}{Var_A^2} \tag{12}$$

$$V_{EPI} = \frac{\sum_{i=1}^{n} |G_{R1} - G_{R2}|_{filterd}}{\sum_{i=1}^{n} |G_{R1} - G_{R2}|_{original}} \tag{13}$$

where μ_A and Var_A represents the mean and variance of pixels in the uniform area A of the image. V_{ENL} is often used to evaluate the despeckling ability, and the larger the value is, the stronger the despeckling ability is. G_{R1} represents the gray value of the neighboring pixels along the edge of the filtered image, G_{R2} represents the gray value of the neighboring pixels along the edge of the original image. V_{EPI} is often used to evaluate the edge perseveration ability. The closer the value is to 1, the stronger the edge perseveration performance is. In the experiments, the A and B areas in Fig. 3a, the C and D areas in Fig. 3b are selected as the ENL evaluation area.

From Table 1, the proposed algorithm shows more obvious advantages in the three homogeneous regions of A, B, and C than the other four algorithms. It can be seen that the higher V_{ENL} is obtained by MSAR-BM3D in region D, but the V_{EPI} of proposed algorithm is highest for two real SAR images which suggests the better ability of edge preservation. This conclusion is consistent with the more complete and clear edge detection image of the algorithm in Figs. 5 and 6

Table 1 Performance evaluation index comparison in real SAR images

Algorithm	V_{ENL}				V_{EPI}	
	Region A	Region B	Region C	Region D	Figure 4a	Figure 4b
SAR-BM3D	755.8	332.0	1703.1	1610.8	0.944	0.771
MSAR-BM3D	3349.5	983.3	10986.1	4542.6	0.952	0.660
NL-CV	2070.0	788.9	3171.9	1001.1	0.449	0.400
IDPAD	600.9	346.4	1934.6	702.8	0.766	0.632
Proposed	6963.8	2742.8	15827.5	2617.9	0.959	0.881

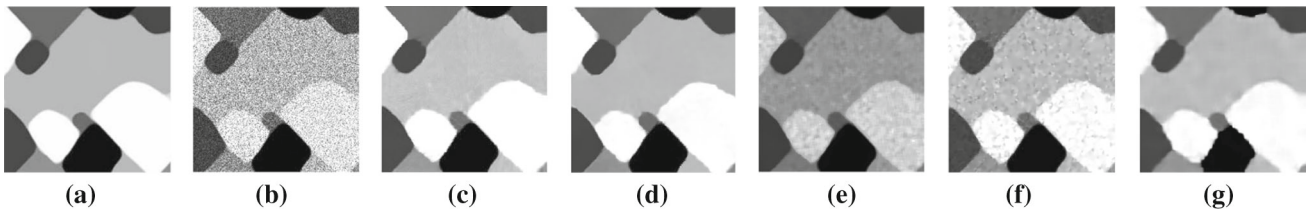

Fig. 7 Despeckling results of simulated SAR image. **a** Original image, **b** simulated SAR image, despeckling results for **c** SAR-BM3D, **d** MSAR-BM3D, **e** NL-CV, **f** IDPAD, **g** proposed method

4.3 Evaluation of synthetic SAR image despeckling

For measuring other quality metrics, noise-free image is simulated by multiplicative noise in Fig. 7a to get a synthetically speckled image in Fig. 7b.

For visual comparison, the despeckled images are in Fig. 7c–g. It is observed that, NL-CV and IDPAD methods' performances are not satisfying which still a great amount of speckle remains. BM3D and MSAR-BM3D implement a valid despeckling effect in synthetic image, which have the obviously smoother homogeneous area. The proposed method provides a good despeckling performance. In terms of edge preservation, it is not as good as c and d in Fig. 7, but still clearer than the other two algorithms.

The Peak Signal-to-Noise Ratio (PSNR) and the structural similarity index measure (SSIM) are used to analyzed the quality of the despeckling result based on denoised image and original image. The greater the value of PSNR and SSIM, the closer the despeckled image to the original image which means better performance of despeckling. According to Table 2, the proposed method shows distinct advantage of SSIM index which means that there is no excessive blurring on the basis of despeckling, and it is basically consistent with the structure of the original image. MSAR-BM3D has the highest value in terms of PSNR, which is consistent with the despeckling result has the smoothest homogeneous area.

Table 2 Performance measure of synthetic SAR image

Algorithm	PSNR	SSIM
SAR-BM3D	26.0038	0.8763
MSAR-BM3D	31.3753	0.8781
NL-CV	29.0461	0.7904
IDPAD	26.9745	0.6973
Proposed	27.5005	0.8817

Table 3 Computational time in seconds

Algorithm	Farmland	Airport
SAR-BM3D	137.819 s	137.607 s
MSAR-BM3D	8.374 s	7.603 s
NL-CV	124.299 s	112.599 s
IDPAD	2.127 s	2.824 s
Proposed	5.068 s	4.865 s

4.4 Computational analysis

As a preprocessing step of SAR image interpretation, the efficiency of the despeckling algorithm is necessary. Table 3 reports the computational time of each method in MATLAB R2016a with Windows 10 operating system on an Intel(R) Core (TM) i5-9500 CPU@ 3.00 GHz, and 8 GB of RAM. IDPAD is obviously the fastest method due to the use of fewer local estimation parameters and smaller window. Among other methods, the proposed algorithm exhibits lowest computational complexity. Therefore, it's more than 20 times faster than the SAR-BM3D and the NL-CV, and almost half of the MSAR-BM3D. Considering the performance of our algorithm, the running time is acceptable for SAR image despeckling and it can be reduced with better hardware.

5 Conclusion

In this paper, a SAR image despeckling method based on reconstructed decay factor and three-stage filtering strategy is proposed. By combining the characteristics of the Lee filter coefficient with the model of the Frost filter, the original decay factor is reconstructed to enhance the ability of edge preservation. In order to give better consideration to both speckle suppression and edge preservation, we used a three-stage filtering strategy.

Firstly, a pre-filtering is performed to abate the speckles, and more accurate local statistical parameters are obtained. Then, the original SAR image is fine-filtered twice by a negative exponential weighting coefficient containing the reconstructed decay factor. Through adjusting the parameters, the results of the two fine filtering are, respectively, giving priority to smooth and edge preservation. Finally, the despeckled image is obtained by weighting two fine-filtered results using the threshold of the reconstructed decay factor. The algorithm in this paper has obvious improvement in visual effect and parameter indicators, meanwhile with the advantages of less complexity compared with advanced despeckling algorithms.

References

1. Soumekh, M.: A system model and inversion for synthetic aperture radar imaging. IEEE Trans. Image Process. **1**(1), 64–76 (1992)
2. Simard, M., Degrandi, G., Thomson, K.P.B., et al.: Analysis of speckle noise contribution on wavelet decomposition of SAR images. IEEE Trans. Geosci. Remote Sens. **36**(6), 1953–1962 (1998)
3. Lee, J.S.: Digital image enhancement and noise filtering by using local statistics. IEEE Trans. Pattern Anal. Mach. Intell. **2**(2), 165–168 (1980)
4. Kuan, D., Sawchuk, A., Strand, T., et al.: Adaptive noise smoothing filter for images with signal-dependent noise. IEEE Trans. Pattern Anal. Mach. Intell. **7**(2), 165–177 (1985)
5. Frost, V.S., Stiles, J.A., Shanmugan, K.S., et al.: A model for radar images and its application to adaptive digital filtering of multiplicative noise. IEEE Trans. Pattern Anal. Mach. Intell. **4**(2), 157–165 (1982)
6. Buades, A., Coll, B., Morel, J.M.: A non-local algorithm for image denoising. In: Proceedings of IEEE Computer Society Conference on Computer Vision and Pattern Recognition, pp. 60–65. San Diego, USA (2005)
7. Dabov, K., Foi, A., Katkovnik, V., et al.: Image denoising by sparse 3-D transform-domain collaborative filtering. IEEE Trans. Image Process. **16**(8), 2080–2095 (2007)
8. Sara, P., Mariana, P., Cesario, V.A., et al.: A nonlocal SAR image denoising algorithm based on LLMMSE wavelet shrinkage. IEEE Trans. Geosci. Remote Sens. **50**(2), 606–616 (2012)
9. Chierchia, G., Gheche, M.E., Scarpa, G., et al.: Multitemporal sar image despeckling based on block-matching and collaborative filtering. IEEE Trans. Geosci. Remote Sens. **55**(10), 5467–5480 (2017)
10. Cozzolino, D., Parrilli, S., Scarpa, G., et al.: Fast adaptive nonlocal SAR despeckling. IEEE Trans. Geosci. Remote Sens. Lett. **11**(2), 524–528 (2014)
11. Chen, S., Hou, J., Zhang, H., et al.: De-speckling method based on non-local means and coefficient variation of SAR image. Electron. Lett. **50**(18), 1314–1316 (2014)
12. Delegable, C.A., Denis, L., Tupin, F., et al.: NL-SAR: a unified non-local framework for resolution preserving (Pol)(In) SAR denoising. IEEE Trans. Geosci. Remote Sens. **53**(4), 2021–2038 (2015)
13. Choi, H., Jeong, J.: Despeckling images using a preprocessing filter and discrete wavelet transform-based noise reduction techniques. IEEE Sens. J. **18**(8), 3131–3139 (2018)
14. Erer, I., Kaplan, N.H.: Fast local SAR image despeckling by edge-avoiding wavelets. SIViP **13**(3), 1071–1078 (2019)
15. Devapal, D., Kumar, S.S., Sethunadh, R.: Discontinuity adaptive SAR image despeckling using curvelet based BM3D technique. Int. J. Wavelets Multiresolut. Inf. Process. **17**(3), 1950016-1-23 (2019)
16. Ji, X., Zhang, G.: Contourlet domain SAR image de-speckling via self-snake diffusion and sparse representation. Multimed. Tools Appl. **76**(4), 5873–5887 (2017)
17. Tian, X., Jiao, L., Zhang, X.: Despeckling SAR images based on a new probabilistic model in nonsubsampled contourlet transform domain. SIViP **8**(8), 1459–1474 (2014)
18. Yu, Y., Action, S.T.: Speckle reducing anisotropic diffusion. IEEE Trans. Image Process. **11**(11), 1260–1270 (2002)
19. Fabbrini, L., Greco, M., Messina, M., et al.: Improved anisotropic diffusion filtering for SAR image despeckling. Electron. Lett. **49**(10), 672–674 (2013)
20. Zhu, L., Zhao, X., Gu, M.: SAR image despeckling using improved detail-preserving anisotropic diffusion. Electron. Lett. **50**(15), 1092–1093 (2014)
21. Li, G., Li, C., Zhu, Y., et al.: An improved speckle-reduction algorithm for SAR images based on anisotropic diffusion. Multimed. Tools Appl. **76**(17), 17615–17632 (2017)
22. Wang, P., Zhang, H., Patel, V.M.: SAR image despeckling using a convolutional neural network. IEEE Signal Process. Lett. **24**(12), 1763–1767 (2017)
23. Yue, D., Xu, F., Jin, Y.: SAR despeckling neural network with logarithmic convolutional product model. Int. J. Remote Sens. **39**(21), 7483–7505 (2018)